

## Supplementary Information

### **Ultra-Deep Blue Thermally Activated Delayed Fluorescence Emitters Constructed by Carbazole Derivatives Enable Efficient Solution- Processed OLED with CIE<sub>y</sub> < 0.05**

Bo Chen,<sup>ab</sup> Chuanxin Liao,<sup>ab</sup> Dewang Li,<sup>\*cd</sup> Hongli Liu,<sup>ab</sup> Shirong Wang<sup>\*ab</sup>

*<sup>a</sup> School of Chemical Engineering and Technology, Tianjin University, Tianjin, 300072, China.*

*<sup>b</sup> Collaborative Innovation Center of Chemical Science and Engineering (Tianjin), Tianjin 300072, China.*

*<sup>c</sup> Joint School of National University of Singapore and Tianjin University International Campus of Tianjin University Binhai New City, Fuzhou 350207, China.*

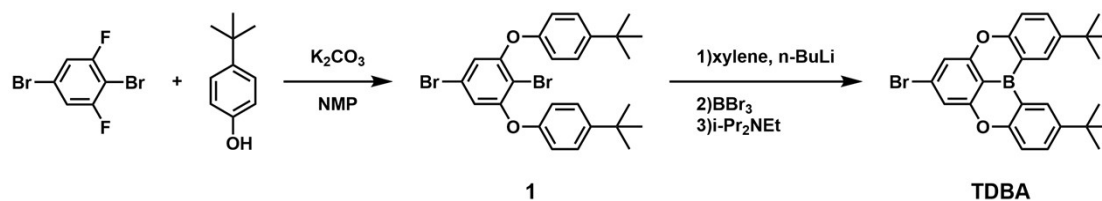
*<sup>d</sup> School of Materials Science and Engineering and Tianjin Key Laboratory of Molecular Optoelectronic Science, Tianjin University and Collaborative Innovation Center of Chemical Science and Engineering (Tianjin).*

#### **Corresponding Author**

*E-mail: [lidewang@tju.edu.cn](mailto:lidewang@tju.edu.cn)*

*E-mail: [wangshirong@tju.edu.cn](mailto:wangshirong@tju.edu.cn)*

## 1. Synthesis



**Scheme S1.** Synthetic routes and structures of TDBA.

### Synthesis of 4,4'-((2,5-dibromo-1,3-phenylene)bis(oxy))bis(tert-butylbenzene) (1)

2,5-Dibromo-1,3-difluorobenzene (2.72 g, 10 mmol), 4-tert-butylphenol (4.51 g, 30 mmol) and  $K_2CO_3$  (4.15 g, 30 mmol) were added to 20 mL anhydrous N-methylpyrrolidone and stirred at 180 °C for 8 hours. The reaction mixture was diluted with dichloromethane and poured into water, then extracted with dichloromethane and combined the organic phase. The organic phase was washed with saturated salt water and dried with anhydrous  $Na_2CO_3$ . After the solvent was removed in vacuum, the crude product was purified by column chromatography (eluent: petroleum ether) to obtain the desired compound 1 (4.70 g, 88.3%) as a white solid.  $^1H$  NMR (400 MHz,  $CDCl_3$ )  $\delta$  7.43 – 7.38 (m, 4H), 7.01 – 6.97 (m, 4H), 6.73 (s, 2H), 1.35 (s, 18H).  $^{13}C$  NMR (101 MHz,  $CDCl_3$ )  $\delta$  156.65, 153.31, 147.45, 126.89, 120.99, 118.74, 116.16, 105.32, 34.43, 31.46. HRMS(APCI) calcd for  $C_{26}H_{29}Br_2O_2$  [M+H] 533.0510, found 533.0510.

### Synthesis of 7-bromo-2,12-di-tert-butyl-5,9-dioxa-13b-boranaphtho[3,2,1-de]anthracene (TDBA)

A solution of n-butyllithium in hexane (2.2 mL, 2.5 M, 5.5 mmol) was slowly added to a solution of 4,4'-((2,5-dibromo-1,3-phenylene)bis(oxy))bis(tert-butylbenzene) (2.66 g, 5 mmol) in anhydrous xylene (20 mL) at -80 °C under argon atmosphere. After keeping the reaction at -80 °C for 1 h, the mixture was stirred at room temperature for 2 h. Then a solution of boron tribromide in toluene (3 mL, 2 M, 6 mmol) was added slowly at -80 °C. After 1h, the mixture was stirred at room temperature for 30 min and at 45 °C for 1 h. Then N,N-diisopropylethylamine (1.29 g, 10.0 mmol) was added at 0 °C. The reaction mixture was stirred at room temperature for 30 min and 135 °C for 20 h, and

then cooled to room temperature. The reaction was quenched with methanol. After the solvent was removed in vacuum, the crude product was purified by column chromatography (eluent: petroleum ether) to obtain the desired compound **TDBA** (1.13 g, 49.0%) as a white solid. <sup>1</sup>H NMR (400 MHz, CDCl<sub>3</sub>) δ 8.71 (d, *J* = 2.5 Hz, 2H), 7.78 (dd, *J* = 8.8, 2.5 Hz, 2H), 7.46 (d, *J* = 8.9 Hz, 2H), 7.34 – 7.31 (m, 2H), 1.49 (s, 18H). <sup>13</sup>C NMR (101 MHz, CDCl<sub>3</sub>) δ 158.35, 157.68, 145.34, 131.69, 130.16, 127.95, 117.99, 111.91, 34.55, 31.52. HRMS(APCI) calcd for C<sub>26</sub>H<sub>27</sub>BBrO<sub>2</sub> [M+H] 461.1287, found 461.1289.

#### **Synthesis of 5-(2,12-di-tert-butyl-5,9-dioxa-13b-boranaphtho[3,2,1-de]anthracen-7-yl)-5H-benzofuro[3,2-c]carbazole (BFCz-TDBA)**

7-bromo-2,12-di-tert-butyl-5,9-dioxa-13b-boranaphtho[3,2,1-de]anthracene (1.38 g, 3 mmol), 5H-benzofuro[3,2-c]carbazole (0.85 g, 3.3 mmol), tris(dibenzylideneacetone)dipalladium(0) (82.4 mg, 0.09 mmol), tri-tert-butylphosphine tetrafluoroborate (104.4 mg, 0.36 mmol), sodium tert-butoxide (0.86 g, 9 mmol) and anhydrous toluene (20 mL) were added to the flask and the reaction was refluxed for 48 h under argon atmosphere. After the solvent was removed in vacuum, the crude product was purified by column chromatography (eluent: petroleum ether: dichloromethane = 10: 1) and recrystallized from dichloromethane and hexane to obtain the desired compound **BFCz-TDBA** (1.37 g, 71.6%) as a white solid. <sup>1</sup>H NMR (400 MHz, CDCl<sub>3</sub>) δ 8.80 (d, *J* = 2.5 Hz, 2H), 8.59 (dd, *J* = 7.4, 1.7 Hz, 1H), 7.99 – 7.93 (m, 2H), 7.81 (dd, *J* = 8.8, 2.4 Hz, 2H), 7.76 (dt, *J* = 8.1, 0.9 Hz, 1H), 7.74 – 7.71 (m, 1H), 7.65 (d, *J* = 8.5 Hz, 1H), 7.54 – 7.44 (m, 7H), 7.39 (td, *J* = 7.4, 1.1 Hz, 1H), 1.53 (s, 18H). <sup>13</sup>C NMR (101 MHz, CDCl<sub>3</sub>) δ 158.70, 158.54, 156.34, 151.16, 145.37, 143.16, 140.78, 140.06, 131.69, 130.28, 125.98, 125.39, 125.01, 122.88, 122.82, 121.45, 121.16, 119.80, 118.09, 118.00, 117.00, 111.70, 110.24, 109.18, 106.76, 105.89, 34.60, 31.55. HRMS(APCI) calcd for C<sub>44</sub>H<sub>36</sub>BNO<sub>3</sub> [M+H] 638.2868, found 638.2868.

#### **Synthesis of 5-(2,12-di-tert-butyl-5,9-dioxa-13b-boranaphtho[3,2,1-de]anthracen-7-yl)-7,7-dimethyl-5,7-dihydroindeno[2,1-b]carbazole (ICz-TDBA)**

7-bromo-2,12-di-tert-butyl-5,9-dioxa-13b-boranaphtho[3,2,1-de]anthracene (1.38 g, 3 mmol), 7,7-dimethyl-5,7-dihydroindeno[2,1-b]carbazole (0.94 g, 3.3 mmol),

tris(dibenzylideneacetone)dipalladium(0) (82.4 mg, 0.09 mmol), tri-tert-butylphosphine tetrafluoroborate (104.4 mg, 0.36 mmol), sodium tert-butoxide (0.86 g, 9 mmol) and anhydrous toluene (20 mL) were added to the flask and the reaction was refluxed for 48 h under argon atmosphere. After the solvent was removed in vacuum, the crude product was purified by column chromatography (eluent: petroleum ether: dichloromethane = 10: 1) and recrystallized from dichloromethane and hexane to obtain the desired compound **ICz-TDBA** (1.46 g, 73.3%) as a white solid. <sup>1</sup>H NMR (400 MHz, CDCl<sub>3</sub>) δ 8.83 (d, *J* = 2.5 Hz, 2H), 8.47 (s, 1H), 8.25 – 8.22 (m, 1H), 7.89 (d, *J* = 7.5 Hz, 1H), 7.83 (dd, *J* = 8.8, 2.4 Hz, 2H), 7.68 (t, *J* = 4.0 Hz, 2H), 7.56 (d, *J* = 8.7 Hz, 2H), 7.50 (s, 2H), 7.47 – 7.28 (m, 5H), 1.56 (s, 6H), 1.53 (s, 18H). <sup>13</sup>C NMR (101 MHz, CDCl<sub>3</sub>) δ 158.75, 158.62, 153.45, 153.34, 145.38, 143.41, 140.89, 140.75, 139.59, 132.85, 131.68, 130.29, 127.05, 126.39, 125.84, 124.04, 123.38, 122.56, 120.53, 120.16, 119.40, 118.03, 111.36, 110.26, 106.71, 104.31, 46.88, 34.61, 31.56, 27.96, 26.91. HRMS(APCI) calcd for C<sub>47</sub>H<sub>43</sub>BNO<sub>2</sub> [M+H] 664.3389, found 664.3383.

**Synthesis of 5-(2,12-di-tert-butyl-5,9-dioxa-13b-boranaphtho[3,2,1-de]anthracen-7-yl)-7-phenyl-5,7-dihydroindolo[2,3-b]carbazole (PidCz-TDBA)**

7-bromo-2,12-di-tert-butyl-5,9-dioxa-13b-boranaphtho[3,2,1-de]anthracene (1.84 g, 4 mmol), 5-phenyl-5,7-dihydroindolo[2,3-b]carbazole (1.46 g, 4.4 mmol), tris(dibenzylideneacetone)dipalladium(0) (109.9 mg, 0.12 mmol), tri-tert-butylphosphine tetrafluoroborate (139.3 mg, 0.48 mmol), sodium tert-butoxide (1.15g, 12 mmol) and anhydrous toluene (20 mL) were added to the flask and the reaction was refluxed for 48 h under argon atmosphere. After the solvent was removed in vacuum, the crude product was purified by column chromatography (eluent: petroleum ether: dichloromethane = 5: 1) and recrystallized from dichloromethane and hexane to obtain the desired compound **PidCz-TDBA** (2.00 g, 70.2%) as a white solid. <sup>1</sup>H NMR (400 MHz, CDCl<sub>3</sub>) δ 8.83 (s, 1H), 8.79 (d, *J* = 2.5 Hz, 2H), 8.26 (dt, *J* = 7.5, 1.7 Hz, 2H), 7.80 (dd, *J* = 8.8, 2.4 Hz, 2H), 7.60 (dd, *J* = 8.3, 1.3 Hz, 3H), 7.56 – 7.48 (m, 5H), 7.43 – 7.30 (m, 8H), 1.52 (s, 18H). <sup>13</sup>C NMR (101 MHz, CDCl<sub>3</sub>) δ 158.69, 158.56, 145.27, 143.57, 141.69, 141.28, 141.21, 140.79, 137.81, 131.57, 130.23, 129.94, 127.41, 126.98, 125.20, 125.11, 124.36, 123.84, 120.45, 119.89, 119.67, 119.64, 119.07,

118.98, 117.98, 111.50, 109.80, 109.42, 106.58, 89.68, 34.58, 31.55. HRMS(APCI)  
calcd for C<sub>50</sub>H<sub>41</sub>BN<sub>2</sub>O<sub>2</sub> [M+H] 713.3342, found 713.3341.

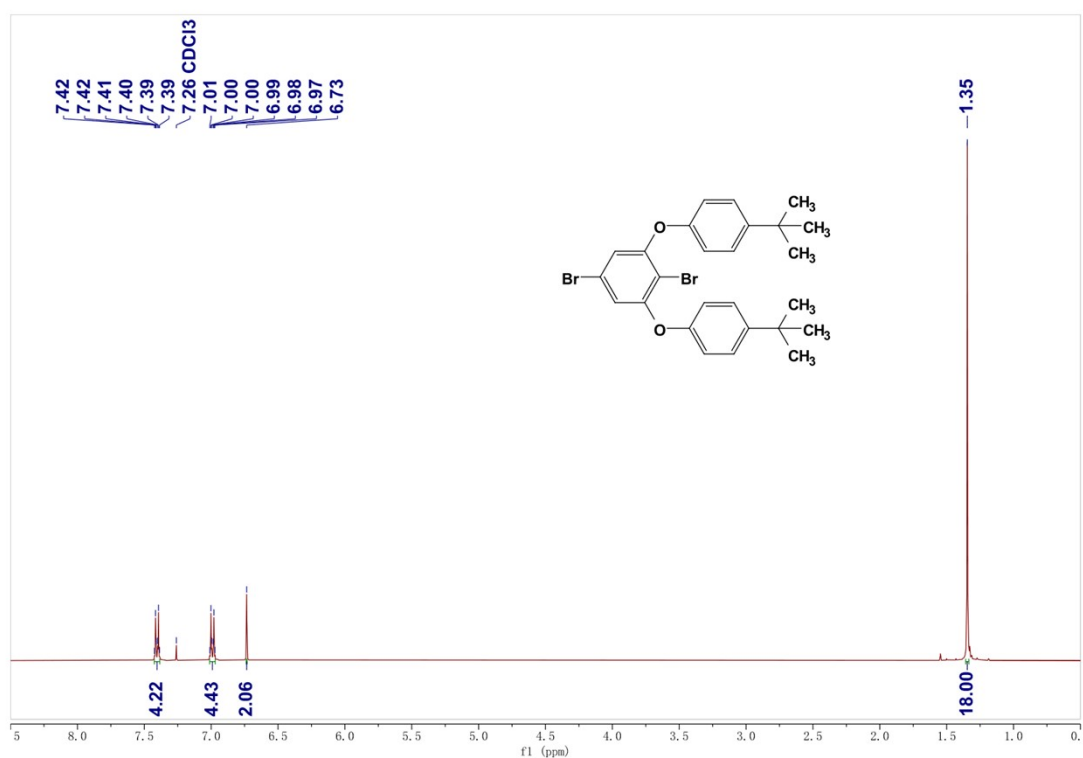


Figure S1. <sup>1</sup>H NMR spectrum of 1.

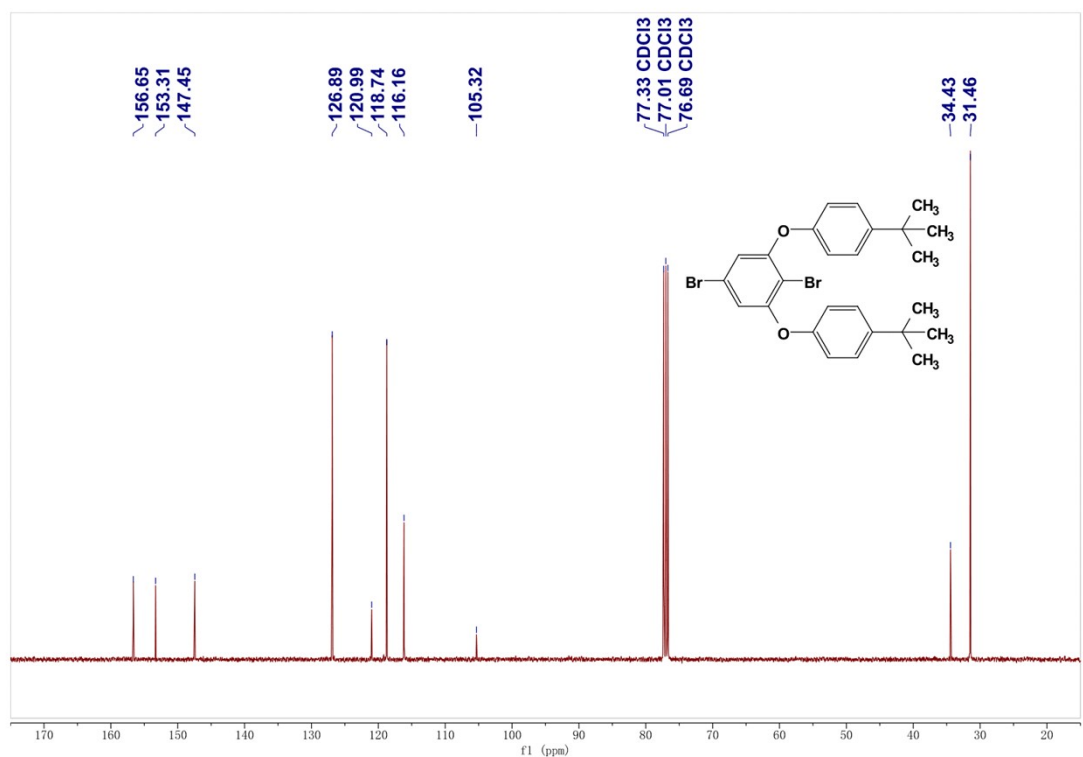


Figure S2. <sup>13</sup>C NMR spectrum of 1.

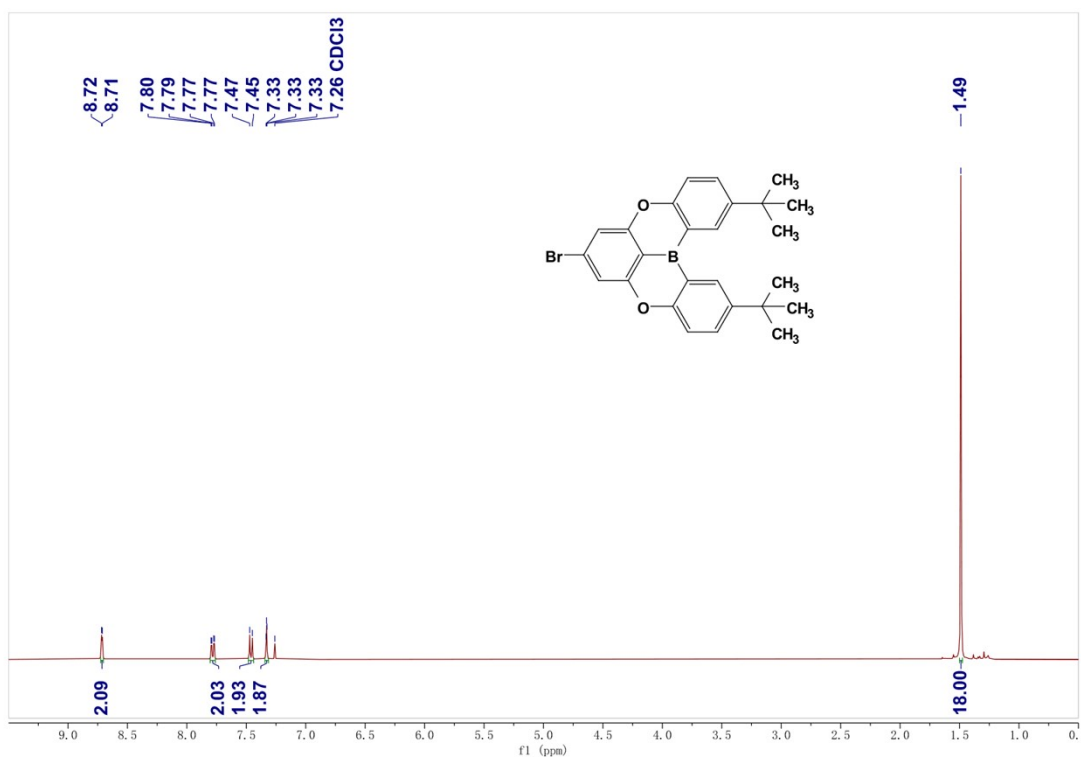


Figure S3.  $^1\text{H}$  NMR spectrum of TDBA.

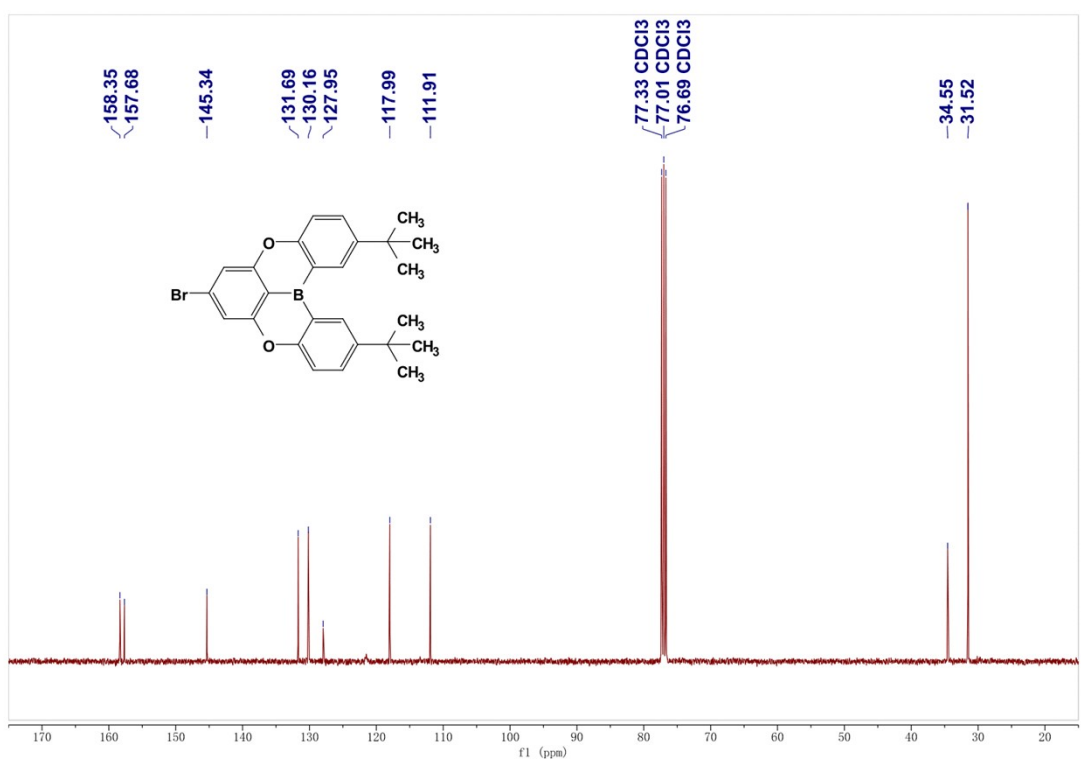


Figure S4.  $^{13}\text{C}$  NMR spectrum of TDBA.

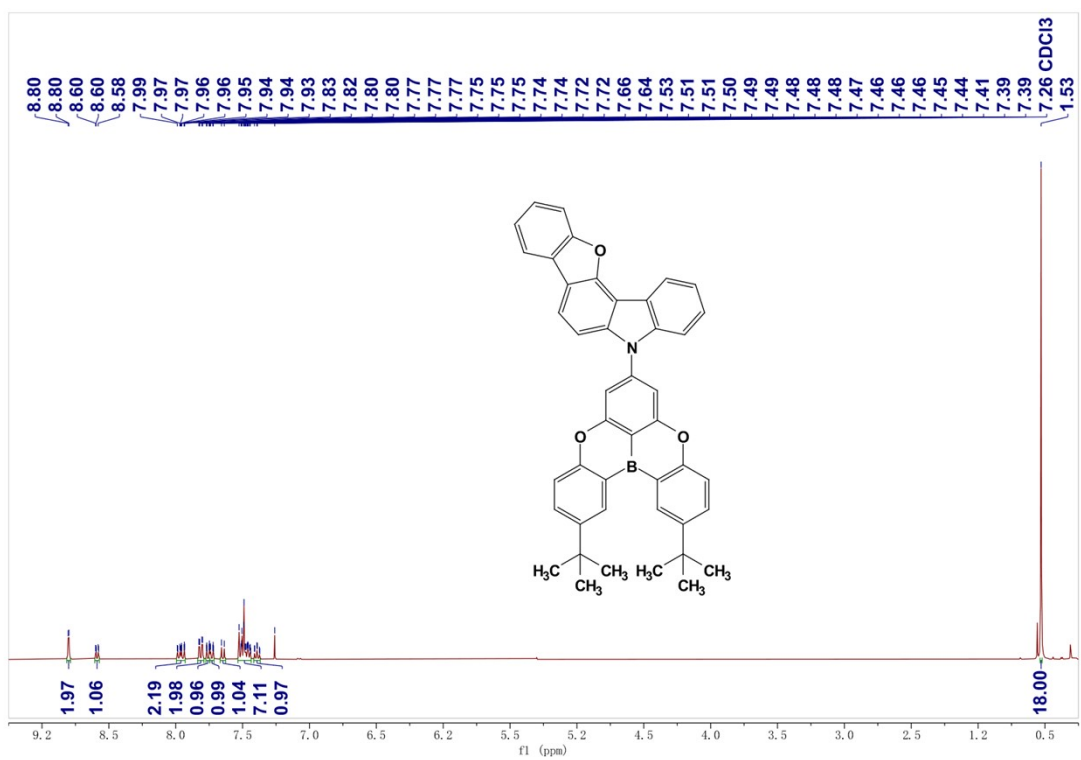


Figure S5. <sup>1</sup>H NMR spectrum of BFCz-TDBA.

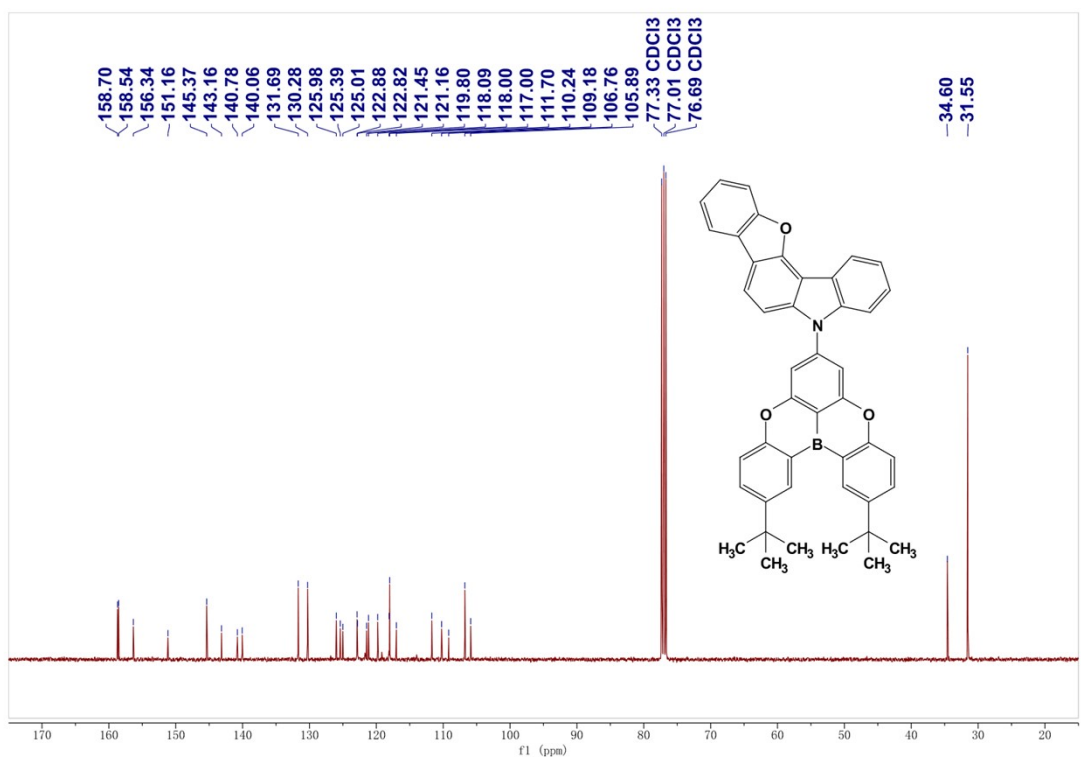


Figure S6. <sup>13</sup>C NMR spectrum of BFCz-TDBA.

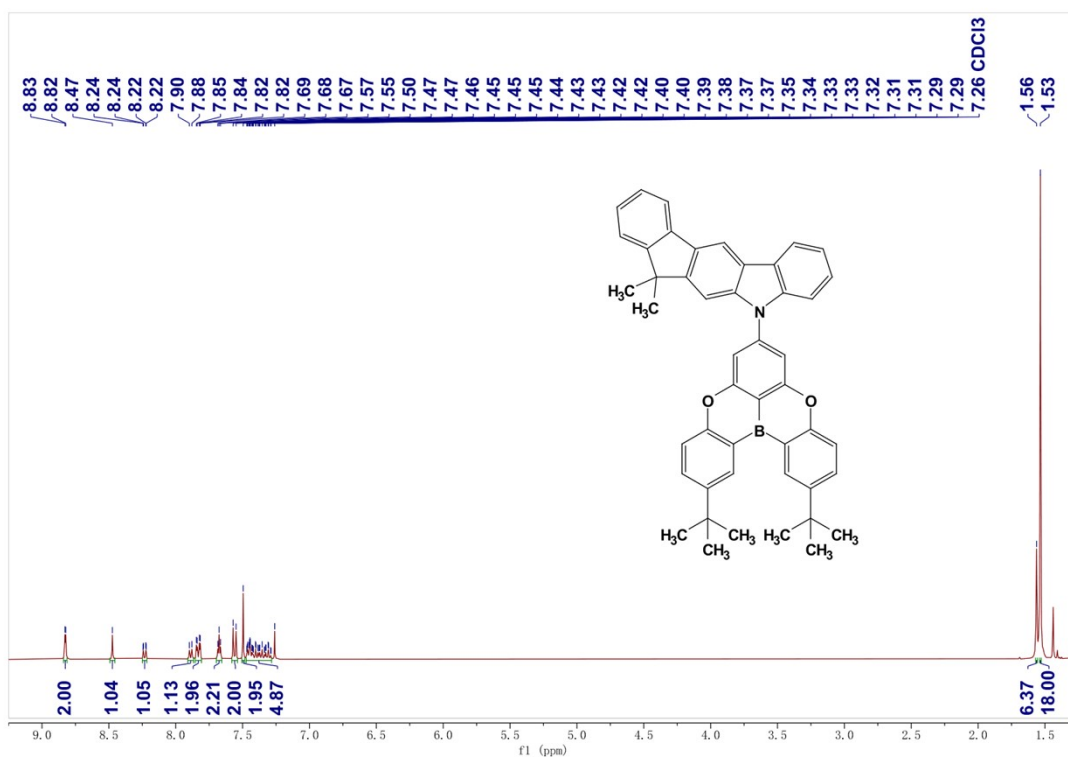


Figure S7.  $^1\text{H}$  NMR spectrum of ICz-TDBA.

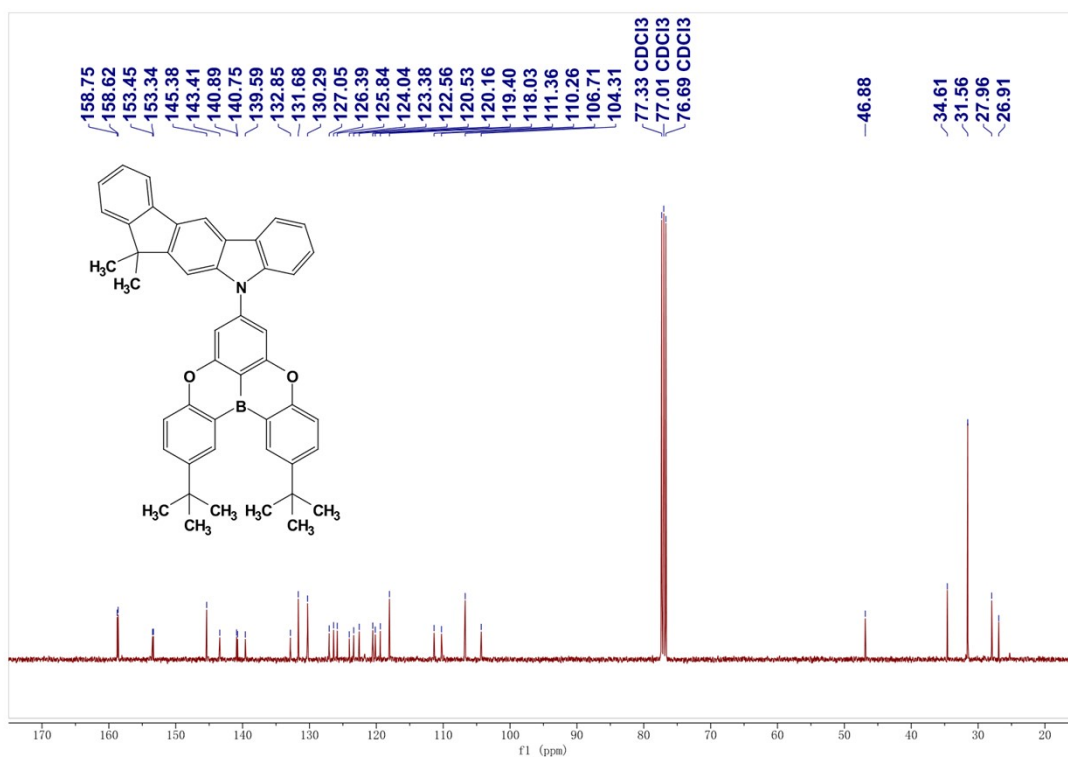


Figure S8.  $^{13}\text{C}$  NMR spectrum of ICz-TDBA.



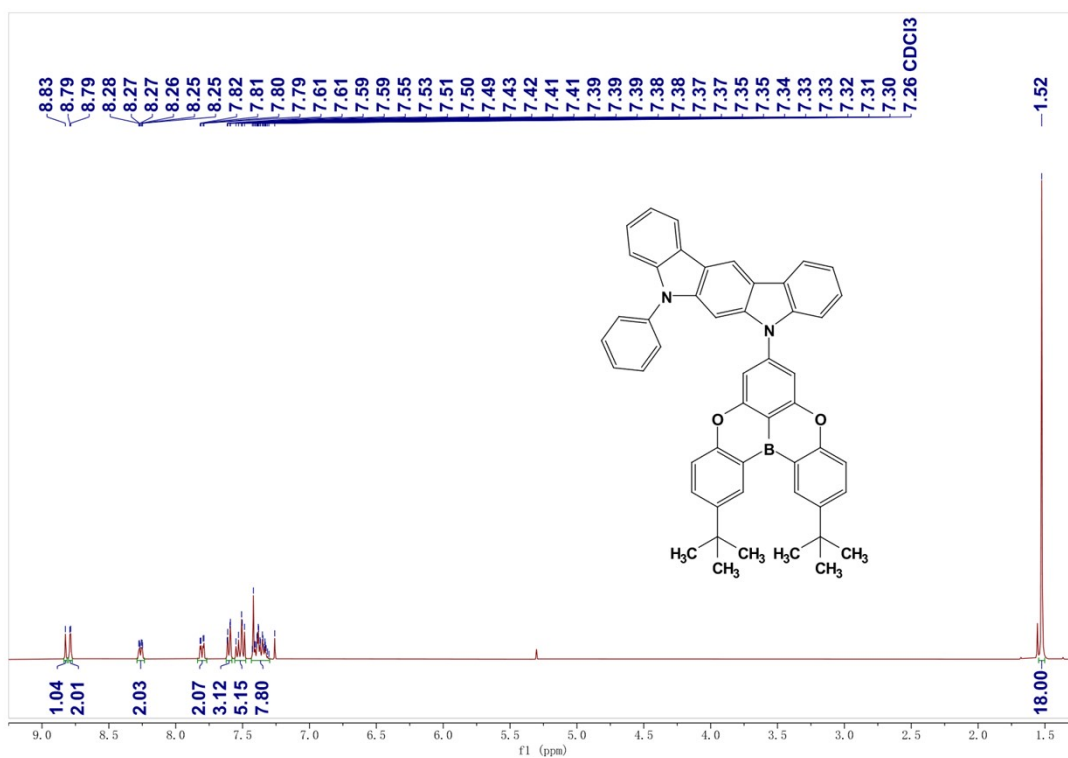


Figure S9.  $^1\text{H}$  NMR spectrum of PIcZ-TDBA.

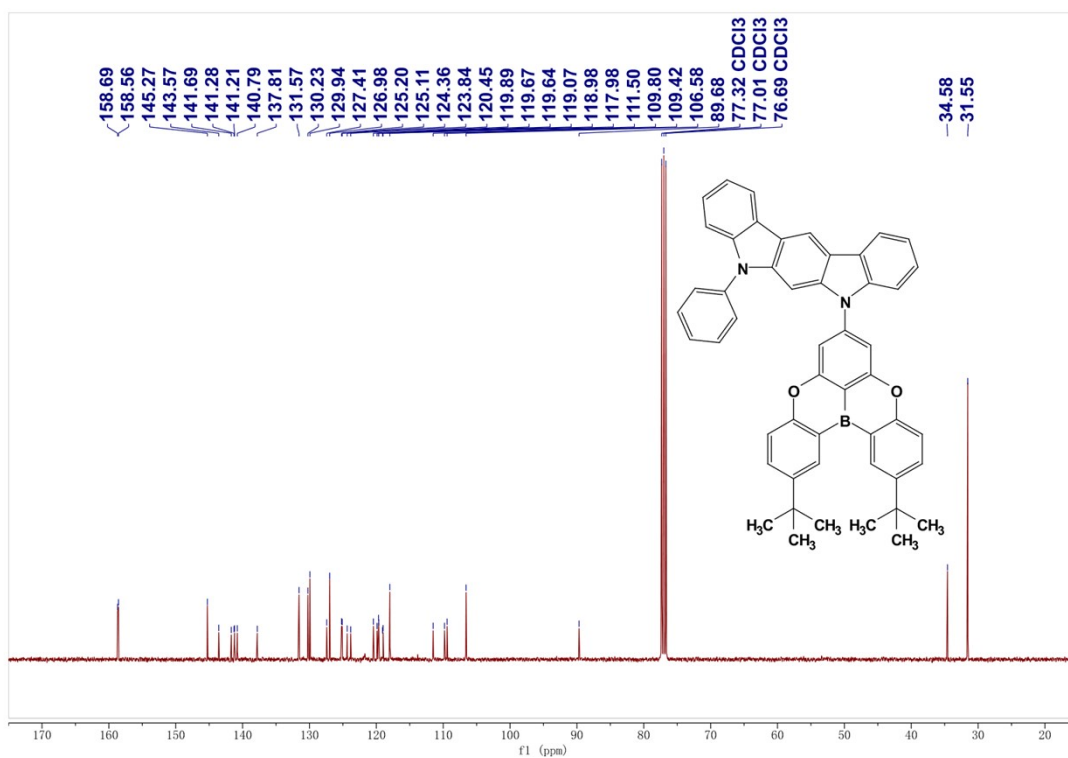
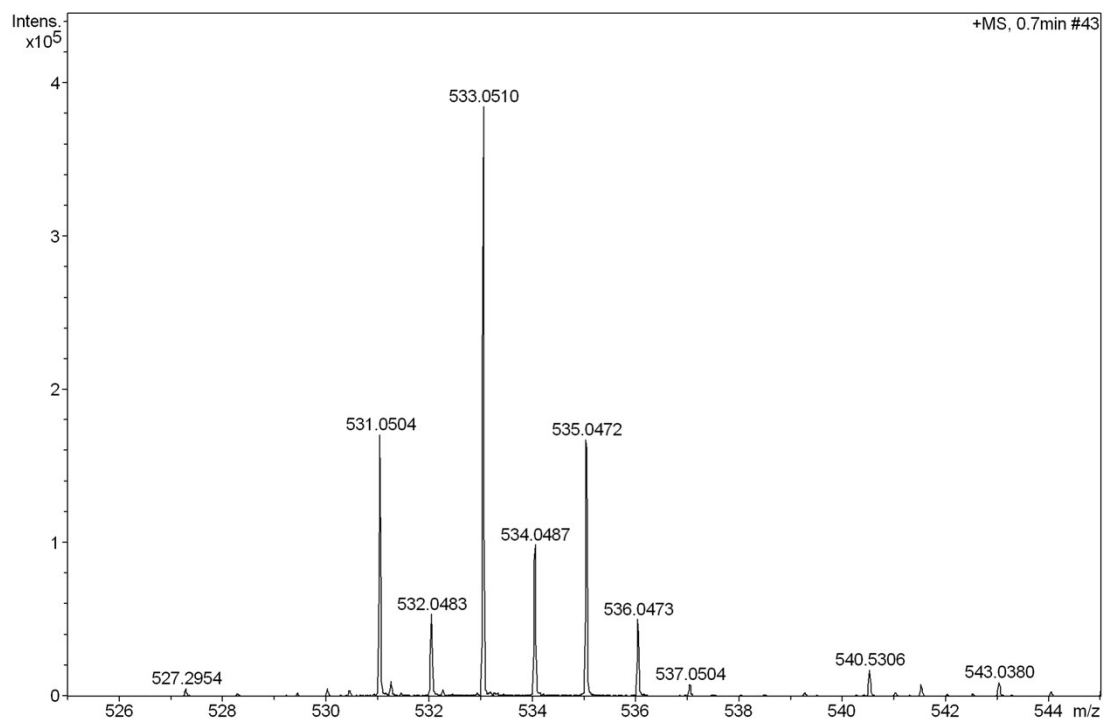
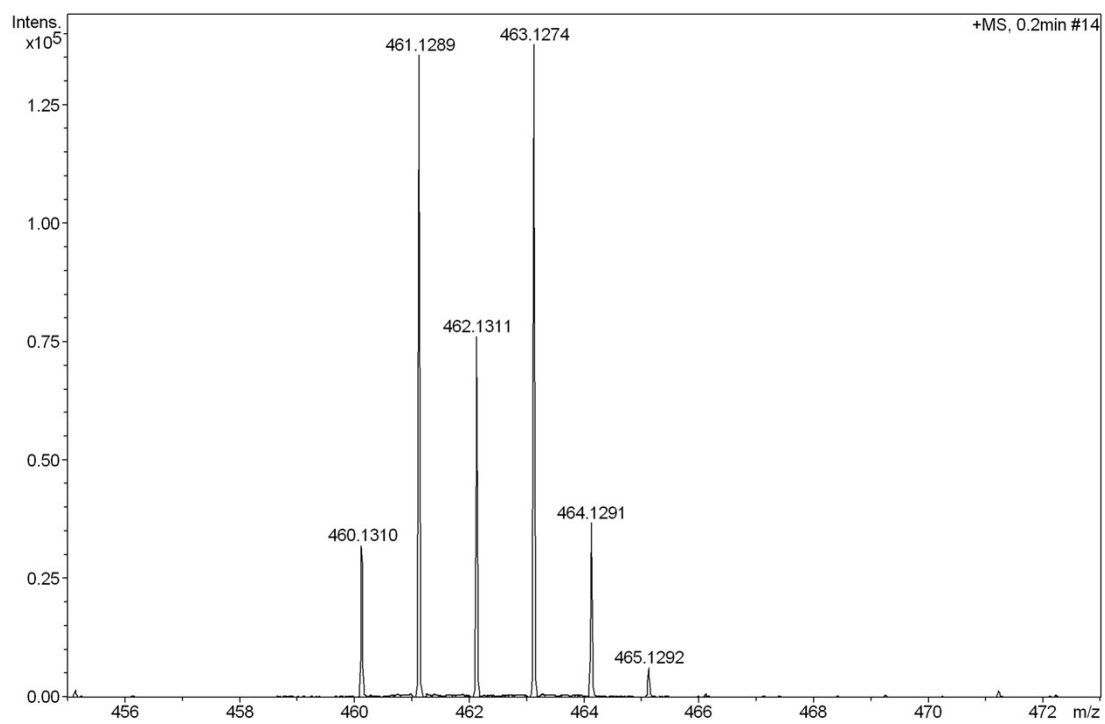


Figure S10.  $^{13}\text{C}$  NMR spectrum of PIcZ-TDBA.



**Figure S11.** HRMS spectrum of **1**.



**Figure S12.** HRMS spectrum of **TDBA**.

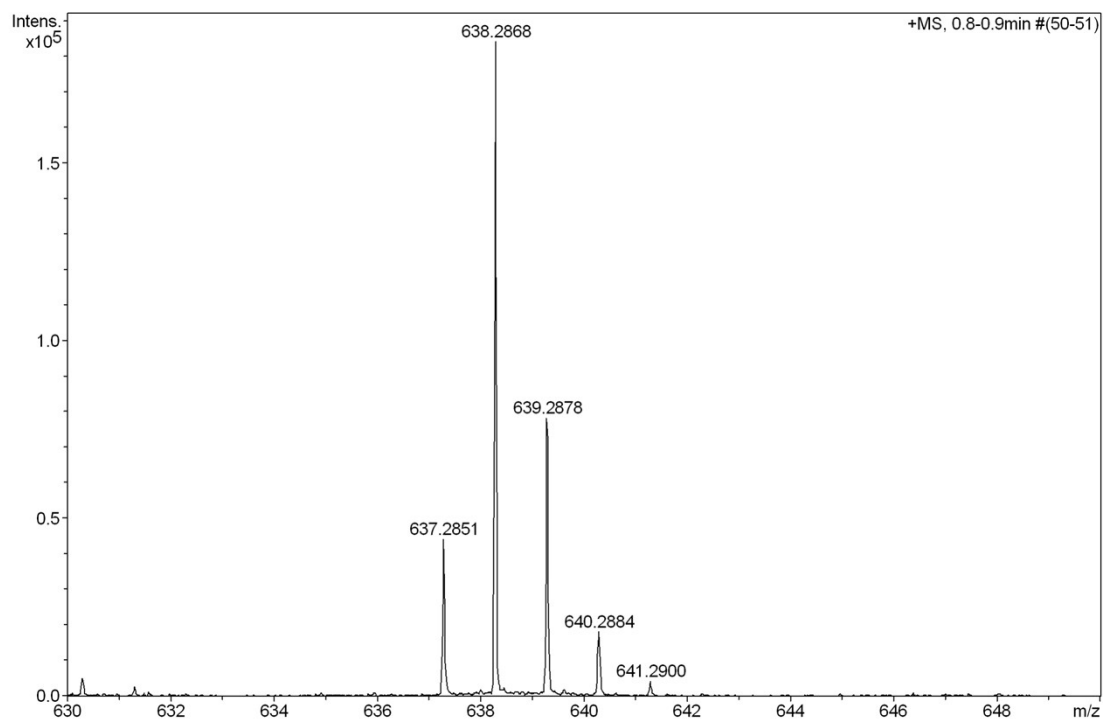


**Figure S13.** HRMS spectrum of BFCz-TDBA.

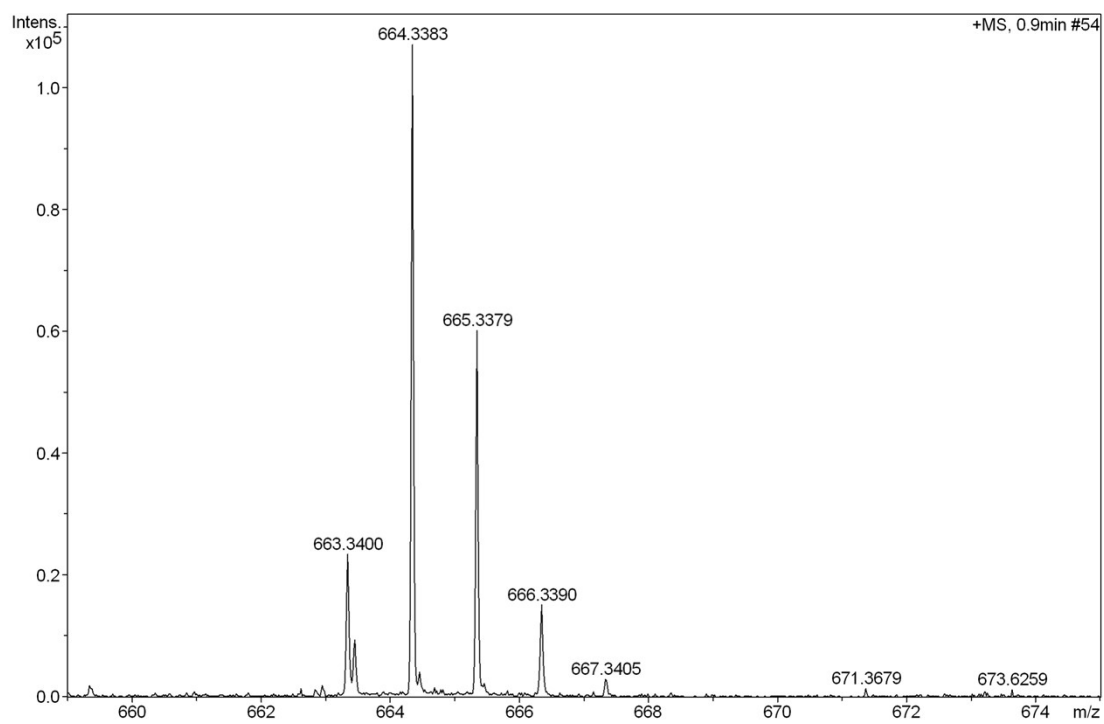


**Figure S14.** HRMS spectrum of ICz-TDBA.

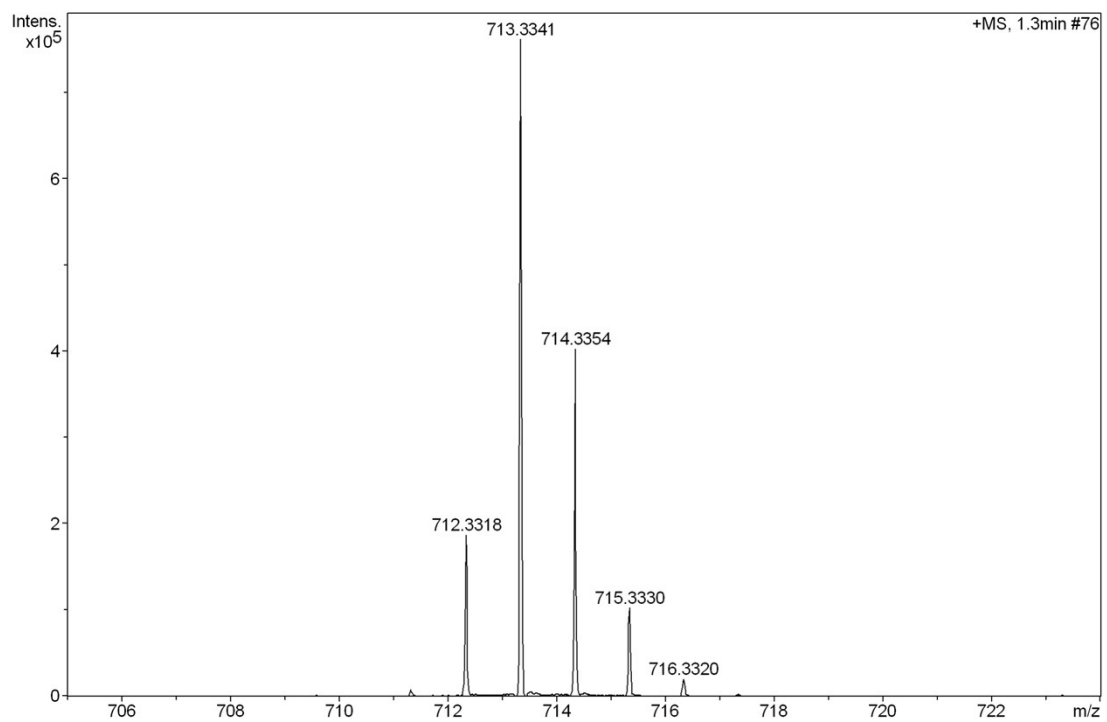


**Figure S15.** HRMS spectrum of **PIdCz-TDBA**.

## 2. Computational Details

All calculations performed to the TADF emitters were implemented using the Gaussian 09 software package. The optimized ground state geometrical configurations and frontier molecular orbitals (HOMO and LUMO) were determined using the density functional theory (DFT) calculations with the B3LYP/6-31G(d) basis set. Excited state energies and natural transition orbitals (NTOs) were calculated using the time-dependent DFT (TD-DFT) with the B3LYP/6-31G(d) basis set.

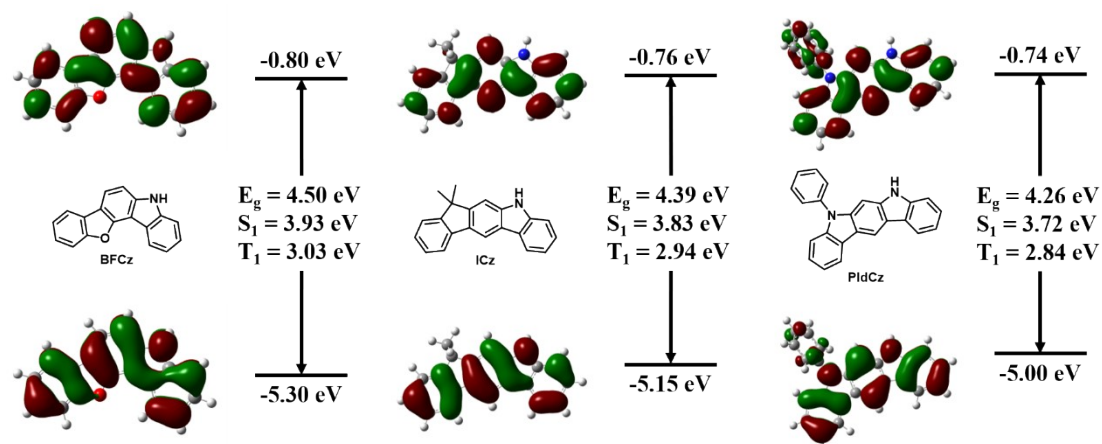


**Figure S16.** Theoretically calculated spatial distributions, singlet and triplet energies, and energies of the HOMO and LUMO levels of BFCz, ICz, and PldCz.

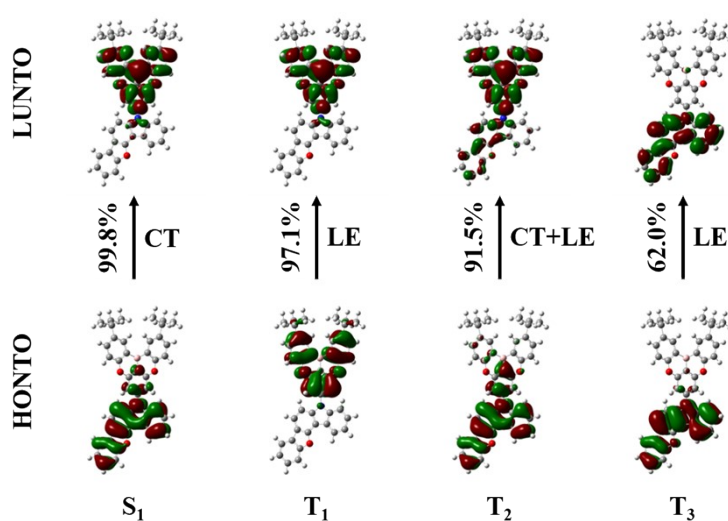


**Figure S17.** Natural transition orbitals (NTOs) for the singlet and triplet states of BFCz-TDBA.

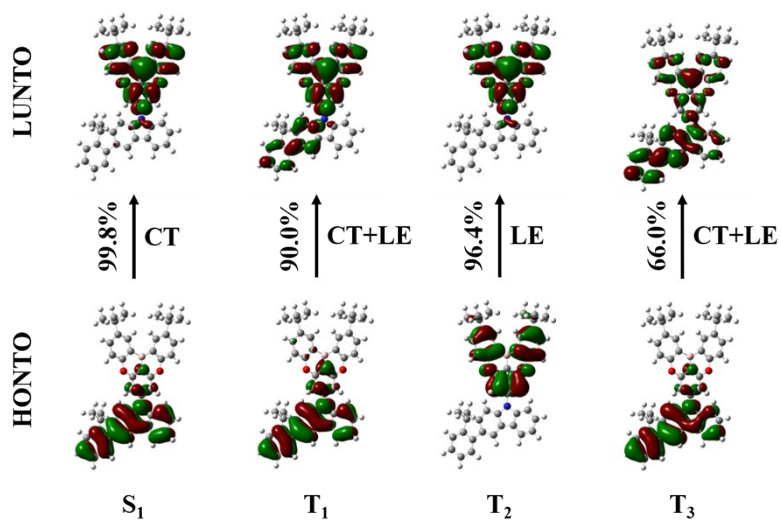


**Figure S18.** Natural transition orbitals (NTOs) for the singlet and triplet states of ICz-TDBA.

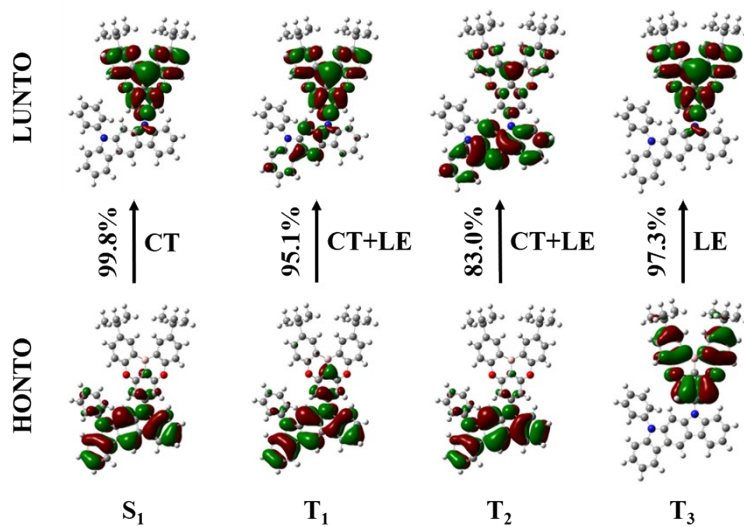


**Figure S19.** Natural transition orbitals (NTOs) for the singlet and triplet states of PIcCz-TDBA.

**Table S1.** Calculated energies of the singlet and triplet states.

Energy [eV]	S <sub>1</sub>	S <sub>2</sub>	T <sub>1</sub>	T <sub>2</sub>	T <sub>3</sub>	T <sub>4</sub>	T <sub>5</sub>
<b>BFCz-TDBA</b>	3.06	3.41	2.88	2.89	3.03	3.32	3.33
<b>ICz-TDBA</b>	2.97	3.41	2.80	2.89	2.97	3.14	3.32
<b>PIcCz-TDBA</b>	2.86	3.04	2.74	2.85	2.89	2.99	3.12

**Table S2.** Energy differences between the singlet and triplet states.

Energy [eV]	$\Delta E_{S1T1}$	$\Delta E_{S1T2}$	$\Delta E_{S1T3}$	$\Delta E_{S1T4}$	$\Delta E_{S1T5}$	$\Delta E_{S2T1}$	$\Delta E_{S2T2}$	$\Delta E_{S2T3}$	$\Delta E_{S2T4}$	$\Delta E_{S2T5}$
<b>BFCz-TDBA</b>	0.18	0.17	0.032	-0.26	-0.27	0.53	0.51	0.38	0.088	0.077
<b>ICz-TDBA</b>	0.17	0.085	0.004	-0.17	-0.35	0.61	0.52	0.44	0.26	0.088
<b>PIcCz-TDBA</b>	0.13	0.011	-0.025	-0.12	-0.26	0.31	0.19	0.16	0.059	-0.078

### 3. Photophysical Properties

#### 3-1 Absorption and photoluminescence spectra

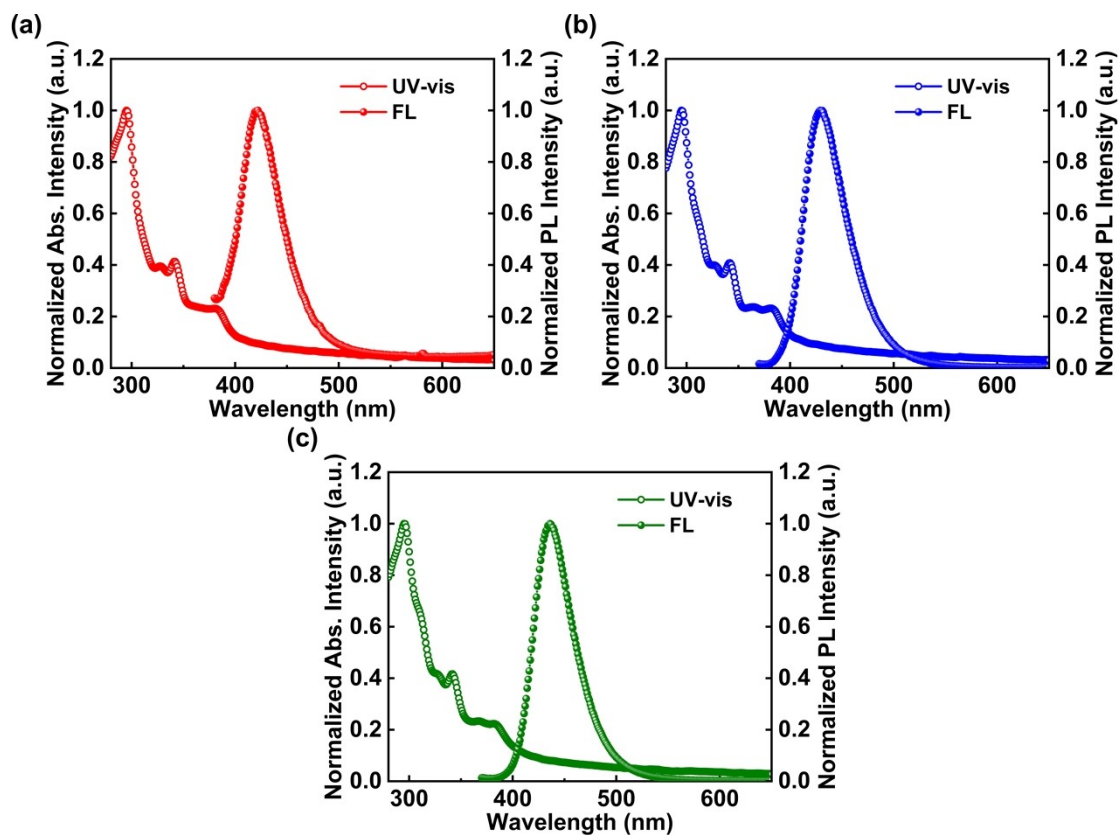


**Figure S20.** Normalized UV-vis absorption and fluorescence (FL) spectra in doped film of (a) BFCz-TDBA, (b) ICz-TDBA, and (c) PIdCz-TDBA.

#### 3-2 Solvatochromic behavior

**Table S3.** Emission peak wavelengths for BFCz-TDBA, ICz-TDBA and PIdCz-TDBA in different polarity solvents.

Emitters	Hexane	Toluene	Tetrahydrofuran	Dichloromethane
	[nm]	[nm]	[nm]	[nm]
BFCz-TDBA	383	393	434	448
ICz-TDBA	385	416	452	471
PIcCz-TDBA	391	424	455	477



### 3-3 Transient PL (TRPL) signals and Kinetic analysis<sup>1</sup>

The kinetic parameters of BFCz-TDBA, ICz-TDBA and PIdCz-TDBA were determined from the experimental data (**Table S4**). The prompt ( $\tau_p$ ) and delayed ( $\tau_d$ ) fluorescence lifetimes were determined by fitting the TRPL signals. In the case where  $k_{nr}^T$  (nonradiative decay from  $T_1$  state) is significantly slower than  $k_{RISC}$  (i.e.,  $k_{RISC} \gg k_{nr}^T$ ),  $k_{nr}^T$  was negligible. The rate constants of radiative decay ( $k_r^S$ ) and nonradiative decay ( $k_{nr}^S$ ) from  $S_1$  to  $S_0$  states, the rate constants of intersystem crossing ( $k_{ISC}$ ) and reverse intersystem crossing ( $k_{RISC}$ ) between  $S_1$  and  $T_1$  states were calculated from the following six equations:

$$k_p = 1/\tau_p$$

$$k_d = 1/\tau_d$$

$$k_r^S = k_p \Phi_p$$

$$k_{ISC} = k_p \frac{\Phi_d}{\Phi_p + \Phi_d}$$

$$k_{nr}^S = k_p \left( 1 - \Phi_p - \frac{\Phi_d}{\Phi_p + \Phi_d} \right)$$

$$k_{RISC} = \frac{k_p \cdot k_d \cdot \Phi_d}{k_{ISC} \cdot \Phi_p}$$

**Table S4.** Quantum Yields, Lifetimes, and Rate Constants of mCP-doped films employing BFCz-TDBA, ICz-TDBA and PIdCz-TDBA.

compounds	$\Phi_{PL}$ [%]	$\Phi_p$ [%]	$\Phi_d$ [%]	$\tau_p$ [ns]	$\tau_d$ [ $\mu$ s]	$k_p$ [ $10^7$ s <sup>-1</sup> ]	$k_d$ [ $10^5$ s <sup>-1</sup> ]	$k_r^S$ [ $10^7$ s <sup>-1</sup> ]	$k_{ISC}$ [ $10^7$ s <sup>-1</sup> ]	$k_{RISC}$ [ $10^6$ s <sup>-1</sup> ]	$k_{nr}^S$ [ $10^7$ s <sup>-1</sup> ]
BFCz-TDBA	58.2	48.9	9.3	5.0	1.31	20.0	7.63	9.78	3.20	0.91	7.02
ICz-TDBA	62.7	51.8	10.9	6.2	0.95	16.1	10.5	8.35	2.80	1.27	4.97
PIdCz-TDBA	54.9	41.8	13.1	7.3	1.15	13.7	8.70	5.73	3.27	1.14	4.70

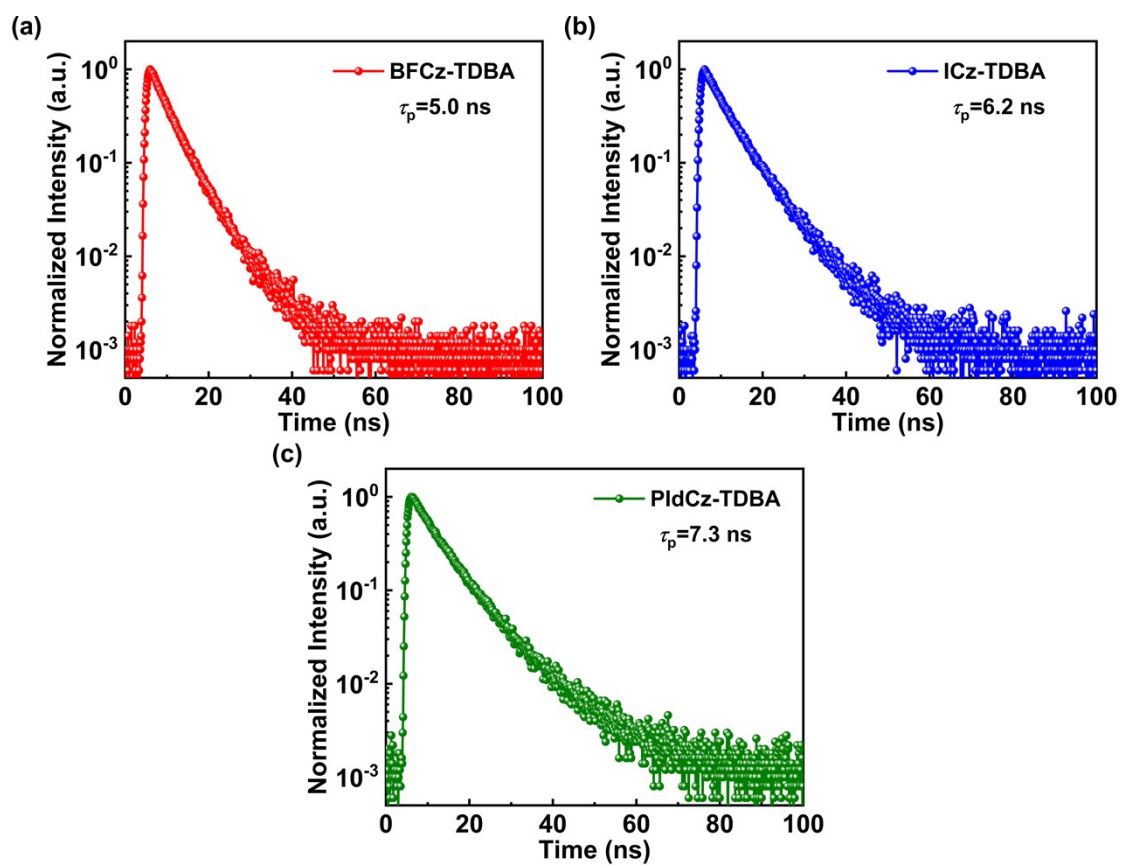


**Figure S21.** Transient photoluminescence decay curves (prompt components) of (a) BFCz-TDDBA, (b) ICz-TDDBA and (c) PIdCz-TDDBA in 20 wt% mCP doped film.

#### 4. Single carrier devices<sup>2</sup>

The single carrier devices of the hole-only device (HOD) and the electron-only device (EOD) using BFCz-TDBA, ICz-TDBA and PIdCz-TDBA were fabricated using the patterned ITO coated glass (serving as the anode) with a sheet resistance of 10.0  $\Omega$ /sq. The HOD and EOD were fabricated with the configuration: ITO/PEDOT:PSS (40 nm)/PVK (10 nm)/mCP: 20 wt% emitters (25 nm)/Al (100 nm) and ITO/ mCP: 20 wt% emitters (25 nm)/TmPyPB (40 nm)/LiF (1 nm)/Al (100 nm), respectively. The PEDOT:PSS and PVK functioned as the hole injecting and transporting layers, respectively, whereas the TmPyPB and LiF functioned as the electron transporting and injecting layers, respectively.

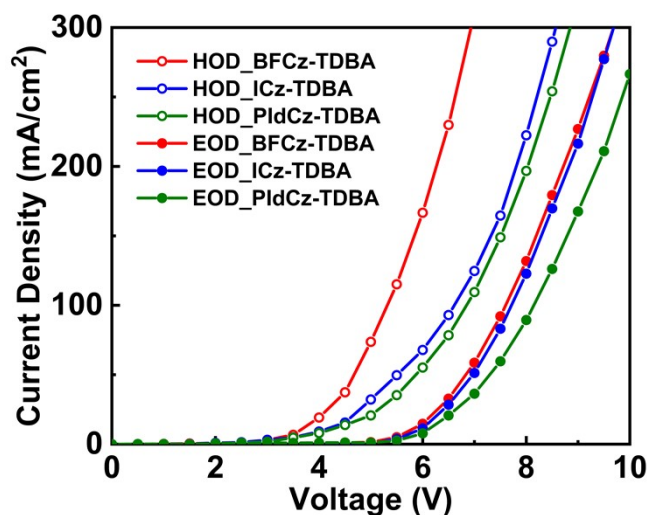


**Figure S22.** Current density-voltage ( $J$ - $V$ ) characteristics of hole-only devices (HOD) and electron-only devices (EOD) of BFCz-TDBA, ICz-TDBA and PIdCz-TDBA.

## 5. Device performance

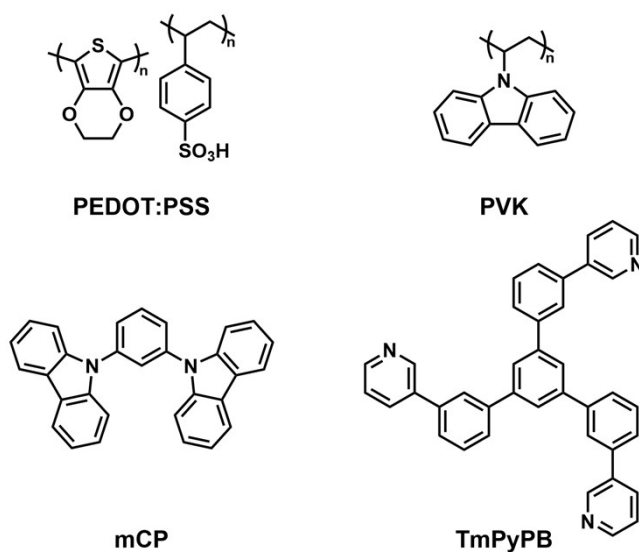


**Figure S23.** Chemical structures of the materials used for the doped deep blue TADF-OLED devices.

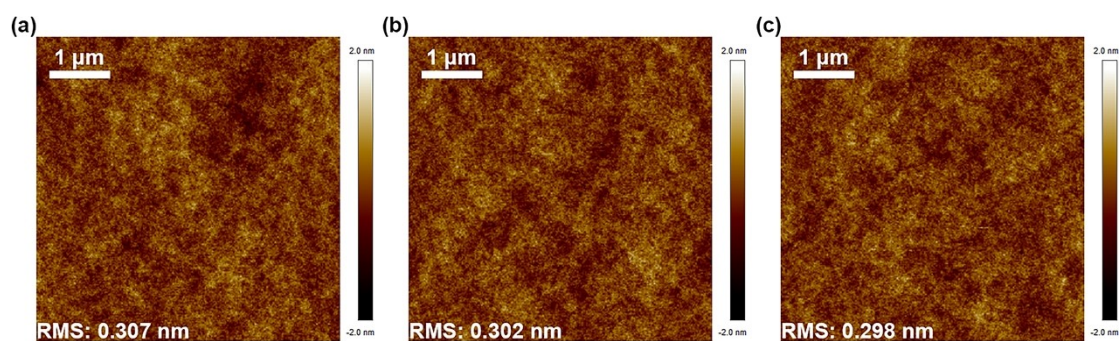


**Figure S24.** AFM height images of the blend films with the mCP host and 20 wt% (a) BFCz-TDBA, (b) ICz-TDBA and (c) PIdCz-TDBA dopants.

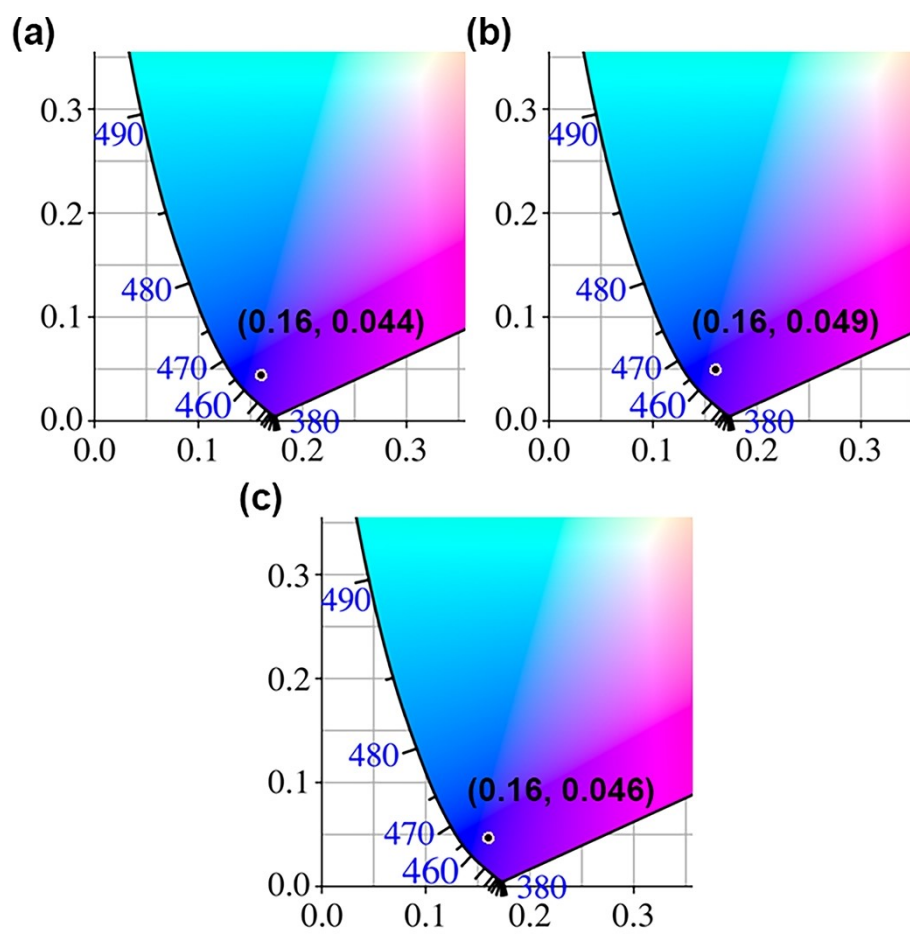


**Figure S25.** CIE 1931 chromaticity diagram of (a) BFCz-TDBA, (b) ICz-TDBA and (c) PIdCz-TDBA.

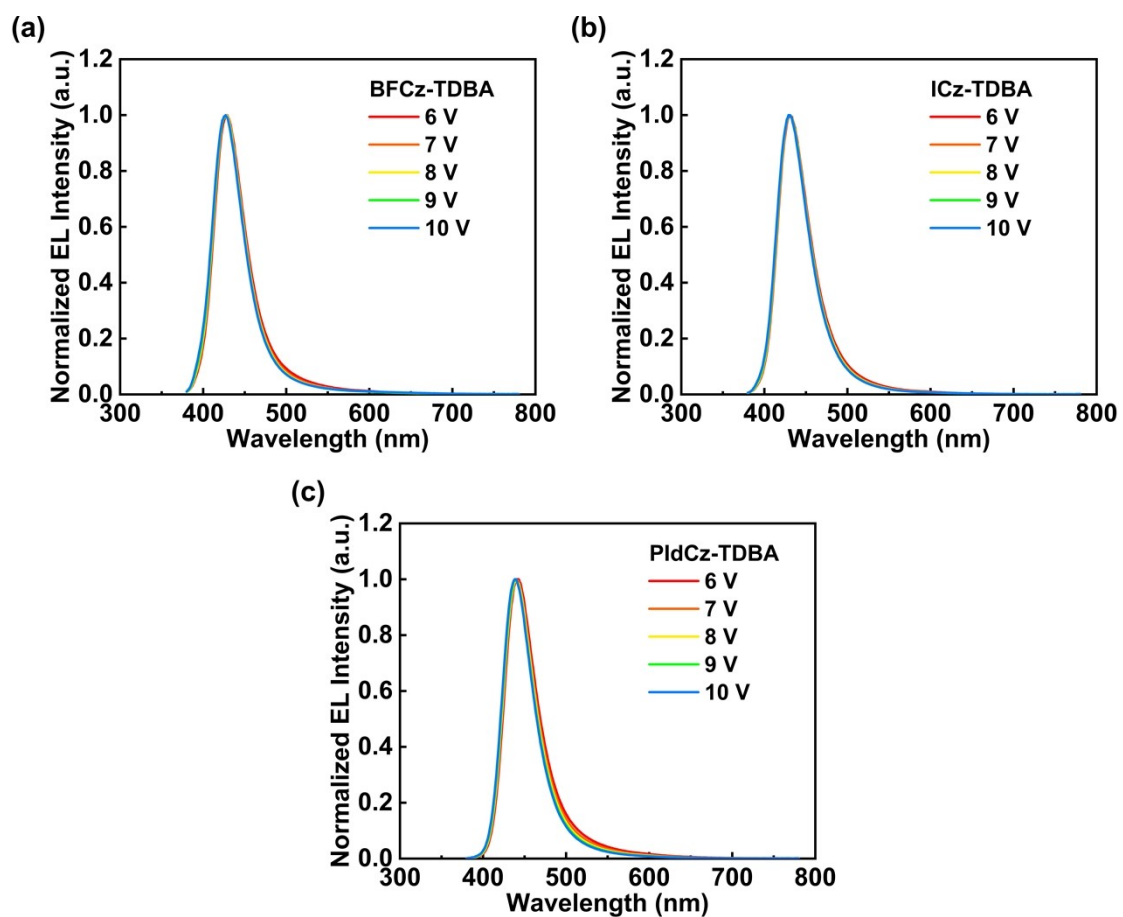


**Figure S26.** Normalized EL spectra of the deep blue TADF-OLED devices of (a) BFCz-TDBA, (b) ICz-TDBA and (c) PIdCz-TDBA from 6 V to 10 V.

## References

1. H. J. Kim, H. Kang, J.-E. Jeong, S. H. Park, C. W. Koh, C. W. Kim, H. Y. Woo, M. J. Cho, S. Park and D. H. Choi, *Adv. Funct. Mater.*, 2021, **31**, 2102588.
2. J. Hwang, C. W. Koh, J. M. Ha, H. Y. Woo, S. Park, M. J. Cho and D. H. Choi, *ACS Appl. Mater. Interfaces*, 2021, **13**, 61454-61462.